Bicontinuous Cubic Morphologies in Block Copolymers and Amphiphile/Water Systems: Mathematical Description through the Minimal Surfaces

Alto D. Benedicto and David F. O'Brien*

Carl S. Marvel Laboratories, Department of Chemistry, University of Arizona, Tucson, Arizona 85721

Received September 26, 1996; Revised Manuscript Received March 6, 1997[⊗]

ABSTRACT: Block copolymers and amphiphile/water systems both exhibit very rich polymorphism. The bicontinuous cubic morphologies mediate the transformation from a lamellar phase to a hexagonally-packed cylinder phase. However, certain bicontinuous cubic morphologies can theoretically transform smoothly (without disruption or tearing) to other bicontinuous cubic morphologies in response to variation in temperature and concentration. These bicontinuous phases are best understood in terms of their associated minimal surfaces. The minimal surfaces D (i.e, ordered bicontinuous double diamond OBDD for block copolymer; cubic phase Q_{224} for amphiphile/water system), G (i.e., gyroid G* for block copolymer; cubic phase Q_{230} for amphiphile/water system), and P (cubic phase Q_{229} for amphiphile/water system; not yet reported for block copolymers) were computed and their two-dimensional projections on the plane reveals various 4-fold and 3-fold symmetries that are at times indistinguishable from that of the hexagonal phase. Moreover, because the surfaces are homotopic, certain 2-D projections of the three bicontinuous cubic phases are remarkably similar. However, the identification of bicontinuous cubic morphologies from each other by various microscopy techniques could still be achieved provided that the number of domains present in an experimental sample is large enough. Experimentally-obtained electron tomographs of sections of suspected bicontinuous phases may be compared with relative ease to the computed slices. These methods extend the range of concentrations in which bicontinuous cubic phases may be classified without the use of X-ray or neutron diffraction since diffractograms are generally difficult to obtain for the dilute samples commonly employed in amphiphile/water systems.

Introduction

Block copolymers are macromolecules composed of blocks of one type of homopolymer attached to another type of homopolymer structure. They represent one of the most useful class of copolymers and behave very differently from random and alternating copolymers. A significant property of block copolymers is their ability to exhibit the properties (e.g., glass transition temperature) of the individual homopolymers.[1] This is due primarily to the general tendency for blocks of the same type to self-aggregate and form domains. Among the most common morphologies resulting from this aggregation are the alternating lamellar phase, the hexagonally-packed cylinders, and the spherical domain structure in cubic lattices.[2] The last 10 years have witnessed the characterization and identification of dramatically different polymer domain morphologies, i.e., the undulating lamellar structure, the catenoid lamellar phase, and various bicontinuous cubic structures, e.g., the OBDD (ordered bicontinuous double diamond) and G* (gyroid).[3−8]

Interestingly, such morphologies have long been observed for amphiphile/water systems.[9−11] Indeed, there appears to be a one-to-one correspondence between the structures observed for block copolymers and that for amphiphile/water systems. Amphiphiles are characterized by having a hydrophilic headgroup attached to a hydrophobic tail. The unfavorable interfacial enthalpic interaction between the hydrophobic tail of the amphiphile with the polar water molecules induces the former to aggregate with the hydrophobic tails of other amphiphiles.[12] The hydrophilic headgroup therefore separates the water from the tail, in much the same way that the A−B junction of a diblock AB copolymer separates the two homopolymer blocks A and B.

For block copolymers, the interactions between the A and B blocks that result in the formation of domains or phases are generally quantified by the Flory−Huggins interaction parameter χ that is a function of temperature.[13,14] In the strong segregation limit ($\chi N >> 10$) (e.g., at low temperature), A and B blocks phase separate, to the extent that the interaction energy between them is primarily localized at their interfacial region.[15] The system is in equilibrium only when the total area of such interface is at a minimum.

This concept of an area-minimizing surface has been used extensively to describe the morphologies in amphiphile/water system. For the same physical reason that soap bubbles assume their particular shape, amphiphile/water systems may exist as micelles, vesicles, hexagonally-packed tubules, lamellar phases, and the more complex bicontinuous cubic phases depending on temperature, concentration, and pressure.[12] The free energy of the system is described by the topology of the surfaces

$$E = \frac{1}{2}\kappa_c \oint (k_1 + k_2 - k_0)^2 \, \mathrm{d}A + \Delta p \int \mathrm{d}V + \lambda \oint \mathrm{d}A \quad (1)$$

where k_1 and k_2 are the principal curvatures while k_o is the spontaneous curvature.[16−18] The spontaneous curvature k_o arises purely as a result of the fact that the dimensions of the microdomain is only a few orders of magnitude greater than that of the constituent molecules (*vide infra*). In other words, the shape of the interface is already influenced by the interactions on a molecular level.[19] If $k_0 = 0$ then the first term of eq 1 is just the square of the mean curvature H ($=(k_1 + k_2)/2$), a well-known quantity used in mathematics.

Clearly, for a system to achieve equilibrium necessitates the minimization of various terms in the free

[⊗] Abstract published in *Advance ACS Abstracts,* May 1, 1997.

S0024-9297(96)01435-0 CCC: $14.00

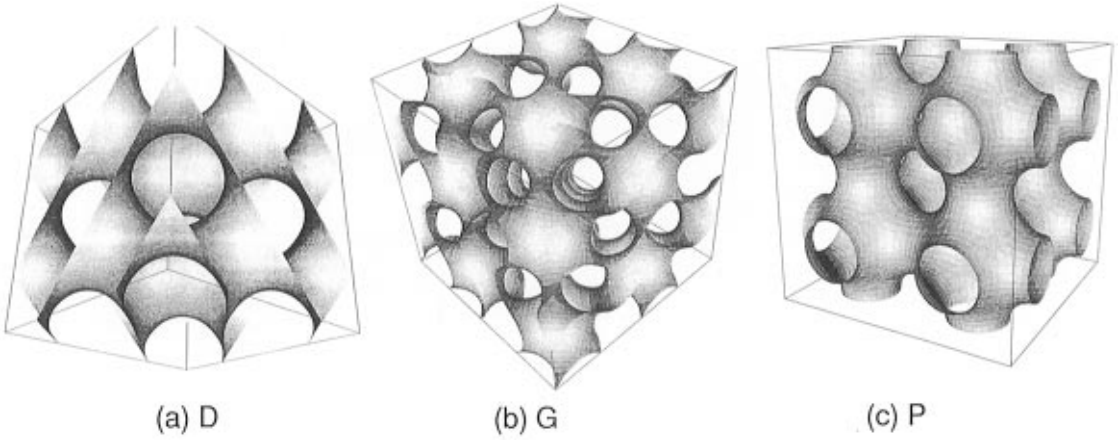

Figure 1. The three minimal surfaces, D, G, and P, that represent the three bicontinuous cubic morphologies found in block copolymers and amphiphile/water systems. These sections are the 2 × 2 × 2 cells of the crystallographic unit cells in Figure 3.

energy expression, chief of which is the mean curvature. Mathematically, this Plateau problem has received a renewed interest in recent years due to the advent of computer graphics. Curiously, the discovery and proof of some new minimal surfaces are partly due to prior graphic visualization of these minimal surfaces that provides sufficient intuition about their characteristics to prove them as such.[20]

The identification of such morphologies for block copolymers and amphiphile/water systems traditionally relies on methods such as X-ray and neutron diffraction scattering (e.g., XRD, SANS),[21] NMR spectroscopy (e.g., diffusion, ^{2}H, ^{31}P),[22] differential scanning calorimetry (DSC), and transmission and scanning electron microscopy (TEM and SEM). With the exception of the various electron microscopy methods, the characterizations are usually indirect.[23] Though space-group identification and unit cell dimensions are readily obtained with diffraction methods, exactly how the molecules are organized in the unit cell for the amphiphile/water system has only been recently settled.[24]

Moreover, the useful range of substrate concentration in which these various characterization methods operate may differ by 2−3 orders of magnitude. For example, the various electron microscopy techniques (TEM, SEM) typically require a much lower amphiphile concentration than is permissible for the various scattering methods (WAXS, SAXS, SANS). X-ray diffraction (XRD) typically requires at least a 200 mM amphiphile solution while TEM and NMR are usually below 75 mM.[25] Since the resultant morphology (or phase structure) depends on concentration, a need arises to be able to determine the morphology at low concentration by techniques other than diffraction or scattering methods.

Chief among these methods is electron microscopy—the traditional TEM and SEM, together with the newer AFM and electron tomography.[26] These methods all rely heavily on visual identification of the morphology of the block copolymer or amphiphile/water system being projected two-dimensionally. With the exception of relatively simple phase structures (such as hexagonally-packed cylinders), more complex phase structures are hard to classify with ease.[23]

This paper presents the first of a series of studies made on the various cubic morphologies in an attempt to make their elucidation by the microscopy techniques easier. In particular, we will focus on just three of the bicontinuous cubic phases as represented by their minimal surfaces, namely, D (i.e, ordered bicontinuous double diamond OBDD for block copolymer; cubic phase Q_{224} for amphiphile/water system), G (i.e., gyroid G* for block copolymer; cubic phase Q_{230} for amphiphile/water system), and P (cubic phase Q_{229} for amphiphile/water system; not yet reported for block copolymers) (Figure 1). The first two structures have already been shown to exist in block polymer morphology.[6−8] The primary reason for such a choice is that these three bicontinuous cubic phases are topologically related (*vide infra*) and belong to single class. It is hoped that such a study would aid in the identification of the final member of this class—the $Im\bar{3}m$.

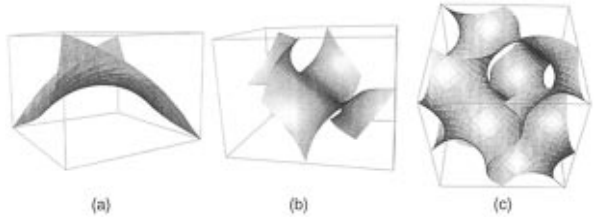

Figure 2. Construction of the minimal surface G.

Experimental (Computational) Section

Calculations were done using a Convex C4620 (Parallel and Serial Processing) with four gigabytes of RAM, and IBM RISC/6000 with 256 MB RAM using Mathematica v2.2.[27] Visualizations were rendered using Geomview[28] (for example, Figure 1) and Cerius2 [29] version 2 (for example, Figure 4) using an Iris Indigo station with Extreme Graphics.

The coordinates $\{x,y,z\}$ of a section of the unit cells (Figure 2a) are generated by solving the hyperelliptic integrals of the following form:[30]

$$x = \mathrm{Re}(e^{i\theta}\int^{\omega}(1-\omega^2)R(\omega)\,d\omega)$$

$$y = \mathrm{Re}(e^{i\theta}\int^{\omega} i(1+\omega^2)R(\omega)\,d\omega)$$

$$z = \mathrm{Re}(e^{i\theta}\int^{\omega} 2\omega R(\omega)\,d\omega)$$

where $R(\omega) = 1/(1 - 14\omega^4 + \omega^8)^{1/2}$ and θ is an association parameter (θ = 0.0, 38.015, and 90.0° for D, G, and P, respectively, and $\omega = u + iv$ is the domain in the complex plane formed from the common intersections of the four circles $(u \pm 1/2^{1/2})^2 + (v \pm 1/2^{1/2})^2 = 2$.

Larger fractions of the unit cells are then constructed using known theorems about the symmetry of minimal surfaces (Figure 2b).[30,31] These fractions now undergo a cell reduction to form the crystallographic unit cells of the minimal surfaces D, G, and P (Figure 2c).

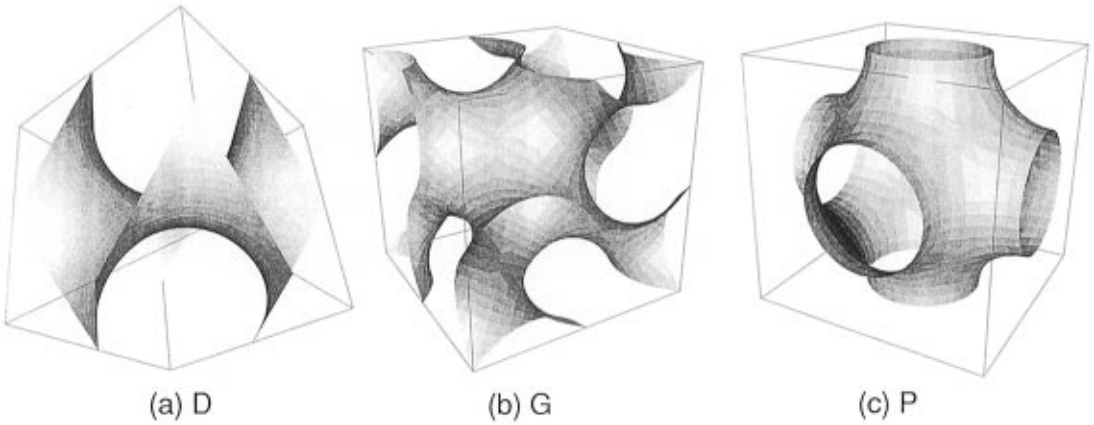

Figure 3. Crystallographic unit cells of the three minimal surfaces for (a) D, (b) G, and (c) P.

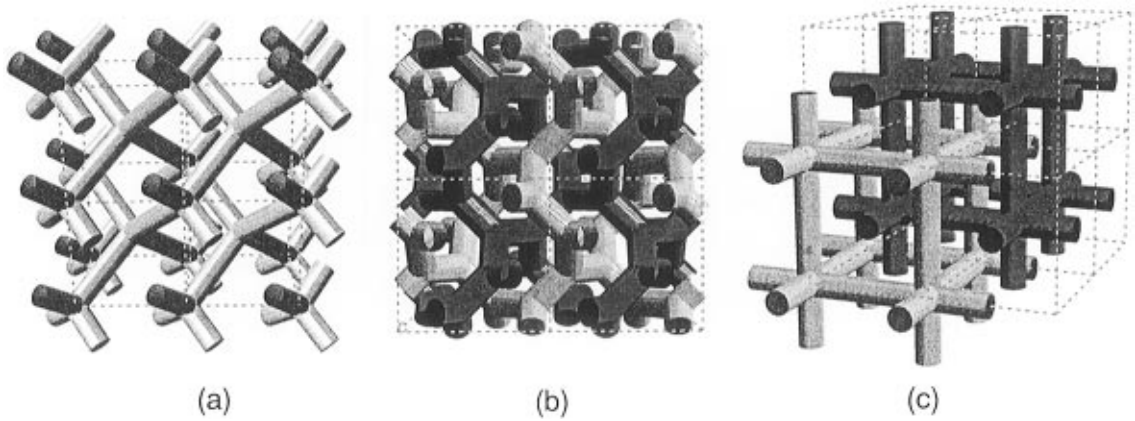

Figure 4. Representation of the three bicontinuous cubic morphologies in three-dimensional labyrinth nets: (a) D; (b) G; (c) P. Note the presence of two uniform labyrinth nets.

Orthographic projections of the minimal surfaces are obtained by slicing through the minimal surfaces. Slices have the thickness of two unit cells.

Results and Discussion

The three chosen bicontinuous cubic morphologies are idealized by the three minimal surfaces: D, G, and P (Figure 1). In the following discussion, we restrict ourselves to the strict definition of a minimal surface being one that has a mean curvature of zero.[32] For amphiphile/water system, the recent consensus is that minimal surfaces are the imaginary surfaces formed by the ends of the hydrophobic tails of the amphiphilic molecules.[33] The surface having least area for a vesicle (subject to fixed inner volume) is therefore a sphere. Though the amphiphiles are usually perpendicular to such a surface, it need not be the case.[12] For AB diblock copolymers, the minimal surfaces are *not* the junctions where the two components A and B comprising the strand of a block copolymer join (since their mean curvature is not zero and it has been the convention to suppose that the A−B junctions lie at a constant nonzero mean curvature[34]). Instead, the minimal surfaces are the midplanes of the microdomains of one of the components of the diblock. To illustrate, for the hexagonally-packed cylinders of A dispersed among the homopolymeric B blocks, the "minimal surface" is a line passing through the middle of each cylinder. This assignment seems supported by the recent TEM micrographs of the gyroid morphology for poly(styrene-*b*-isoprene) and the OBDD morphology for poly(styrene-*b*-butadiene).[6,8]

The minimal surfaces D, G, and P have the basic unit cells with cubic symmetry shown in Figure 3. When amphiphiles are present in such cells, the resultant space groups are $Pn\bar{3}m$, $Ia\bar{3}d$, and $Im\bar{3}m$. From such unit cells, larger surfaces are easily constructed (e.g, 2 × 2 × 2 cells of Figure 1). These surfaces partition space into two identical regions, hence the term bicontinuous. A representation of these two regions in terms of labyrinth nets (formed from this partitioning of space by the minimal surface) illustrates the similarity of the two regions (Figure 4). For amphiphile/water system, these two regions (i.e., nets or "channels") are filled with water molecules. For AB diblock copolymers, these two identical regions are composed of the B block of the copolymer (where B usually has a lower glass transition temperature than the A block).

For the P surface ($Im\bar{3}m$ space group), the second channel (i.e., one of the net or region that resulted from the partitioning of space by the minimal surface) is exactly identical to the first channel, except that it is translated (Figure 4c). Each channel is composed of a "network" of six "tubes" intersecting at a vertex. For a water molecule in an amphiphile/water system, the shortest path along the channel that a water molecule has to travel to complete a cycle will pass through four vertices. Mathematically, each channel in P is a uniform (4,6) net.[35,36]

The G surface ($Ia\bar{3}d$ space group) divides space into two regions that are *mirror images* of each other. *It should be emphasized that the two chiral channels arise from the nature of the deformation of the minimal surface G which is itself not chiral.* However,

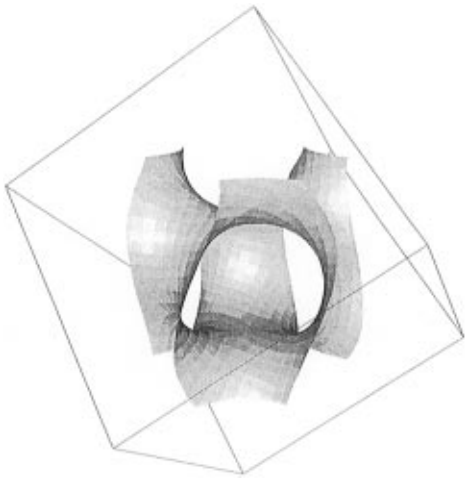

Figure 5. Fraction of the minimal surface G showing the trigonal symmetry.

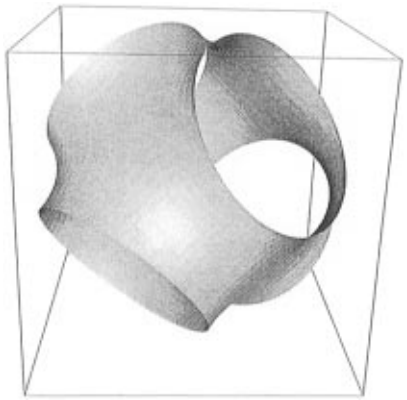

Figure 6. Fraction of the minimal surface D showing the tetrahedral symmetry.

finite sections of surface G are chiral. This is analogous to meso compounds containing asymmetric carbons. Whether the chiral channel can induce local chirality effects depends on the characteristic length scale of the probe molecule.[37] Each of the two channels is composed of a "network" of three "tubes" intersecting at a vertex (Figure 5). The three tubes are 120° of each other and lie on a plane. For the amphiphile/water system, the shortest path along the channel that a water molecule has to travel to complete a cycle will pass through 10 vertices. Mathematically, each channel in G is a uniform (10,3)a net (Figure 4b).

Lastly, for the $Pn\bar{3}m$, the two channels resulting from the partitioning of space by the minimal surface are exactly alike, with one translated from the other. Each channel is a network composed of four tubes emanating from a vertex at 109.5° from each other; hence, the connectivity is similar to that of bonds in diamond (Figure 6). For the amphiphile/water system, the shortest path along the channel that a water molecule has to travel to complete a cycle will pass through six vertices. Each channel forms the familiar "cyclohexanic" diamond structure. Mathematically, each channel in D is a uniform (6,4) net (Figure 4a).

Relationship between the Three Surfaces. Bicontinuous cubic phases generally mediate the transformation of a lamellar phase (in a diblock copolymer or amphiphile/water system) to a hexagonally-packed cylinder phase, in response to temperature or concentration changes in the system.[9] The process clearly involves a disruption of the minimal surfaces associated

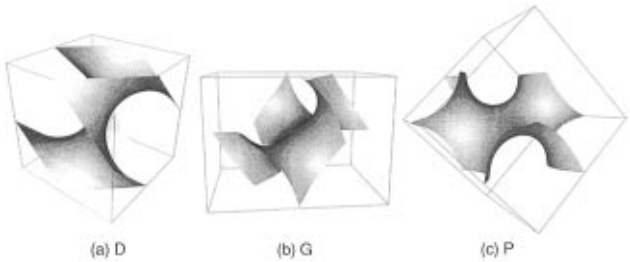

Figure 7. Bonnet transformation of sections of the three minimal surfaces (a) D, (b) G, and (c) P. Bending of D (without "tearing", or stretching) results in G, and further bending results in P. For these three surfaces, D, G, and P, the intermediate surfaces contain self-intersections when Bonnet transform is used.

with each of these phases. However, a given bicontinuous cubic phase may undergo a transformation into another bicontinuous cubic phase without physical disruption if the minimal surfaces of the two bicontinuous cubic phases are related by a continuous homotopy (i.e., the surfaces can be slowly and smoothly deformed into each other).

Topologically, the three minimal surfaces P, G, and D are related by the Bonnet transformation, an isometric mapping of minimal surfaces.[30,31] Without "tearing" or stretching of the surface, the minimal surface P may be bent in such a way as to form a G surface.[38] Further bending results in surface D. Such a bending may easily be seen by taking a small fraction of each of the minimal surfaces (Figure 7). In physical terms, isometry means that the distances between the individual molecules remain the same; i.e., on a local level, the potential energies that are functions of intermolecular distances would remain unchanged. Thus isometry, coupled with the fact that the surfaces remain minimal would imply very small enthalpy difference between the surfaces. However, *Bonnet transformation does not preclude self-intersection of the surface.*[39] In particular, there are countably infinite self-intersecting surfaces that are generated while the three surfaces P, G, and D are Bonnet-transformed into each other.[40] Surface intersection implies that constituent molecules defining the minimal surface intersect each other—a thermodynamically very unfavorable process.

We can show that there is still a continuous homotopy between the surfaces D, G, and P, without invoking the Bonnet transformation.[41] The process is best visualized by examining the behavior of the labyrinth nets (arising from the partitioning of space by the minimal surface) as the minimal surfaces are transformed into each other (Figure 4). The nonintersection of the labyrinth nets in the homotopic transformation implies the existence of a nonintersecting surface separating these nets. Figure 8 shows one possible transformation of the (6,4)-net from the D surface into the (10,3)a-net of the G surface.[42] A similar transformation from P to G can be achieved by similar analysis; thus, all three surfaces P, G, and D are homotopic.[43] *It is important to note that in a continuous homotopic transformation, the intermediate surfaces need not be minimal or isometric.* We propose that it is for this particular reason that intermediate surfaces are not observed when one bicontinuous cubic phase is transformed into another, since the intermediate structures have higher energies than the three bicontinuous cubic structures (*vide infra*).

The existence of a continuous homotopic tranformation gives rise to very interesting consequences for the construction of the phase diagram of both the block

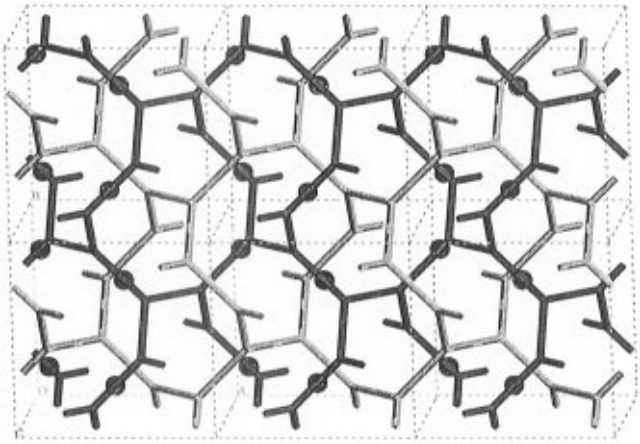

Figure 8. Resultant (10,3) labyrinth net (associated with G) from the (6,4) labyrinth net (associated with D). The circular dots mark the new "edges" that are created by "pulling apart" a tetrahedral vertex to form two trigonal vertices. For clarity, only one of the two intertwining labyrinth nets is labelled with dots.

copolymers and the amphiphile/water systems. For example, it is known that Schoen's normalized surface/volume increases from P to D to G.[40] In the case of amphiphile/water system, this means that $Ia\bar{3}d$ requires the least amount of water, that $Pn\bar{3}m$ requires more water, and finally, $Im\bar{3}m$ requires the most.[44,45] This accounts for the observation that the D phase is usually formed at a higher water concentration than the G phase for various lipid/water systems.[37] Moreover experimentally, if the homotopic transformation were to differ slightly from a Bonnet transformation, then by changing the chemical composition of the amphiphile/water system (e.g., adding more water), *the $Pn\bar{3}m$ structure can be induced to go into $Im\bar{3}m$ merely through a twist of the surface*—without any breakage and reassembling of the aggregate molecules. In the process, *the change in $Pn3m$ to $Im\bar{3}m$ must necessarily pass through the $Ia\bar{3}d$ phase.* Again, this suggests that the rare observance of $Im\bar{3}m$ might be due to the structure being kinetically trapped in the $Pn\bar{3}m$ phase, to prevent the transient formation of the thermodynamically very unfavorable $Ia\bar{3}d$. Similar effects should also be observed for AB block copolymers as the relative fractions of blocks A and B are varied.

Two-Dimensional Projections on a Plane. In order to better understand the three bicontinuous cubic phases as might be seen experimentally through various microscopy methods (e.g., SEM and AFM), slices of the three minimal surfaces D, G, and P along different Miller planes were computed (Figures 9−11). Each slice has the thickness of two unit cells. The absolute length scale of the slices taken from a given minimal surface should not be compared directly to those of another minimal surface as the volumes of the unit cells for different minimal surfaces are not the same.

The high symmetry inherent to the space groups $Pn\bar{3}m$, $Ia\bar{3}d$, $Im\bar{3}m$ in which surfaces D, G, and P belong to, respectively, is evident from the presence of various 4-fold and 3-fold symmetries in a large number of slices. These correspond to the screw axes and glide planes.

Many symmetry elements are shared by these three space groups; thus, several of the slices for the different minimal surfaces are strikingly similar. For instance, P(100) looks like G(100), while D(110) looks like P(110). In particular, $Pn\bar{3}m$ is a subgroup of index 2 to $Im\bar{3}m$.[46]

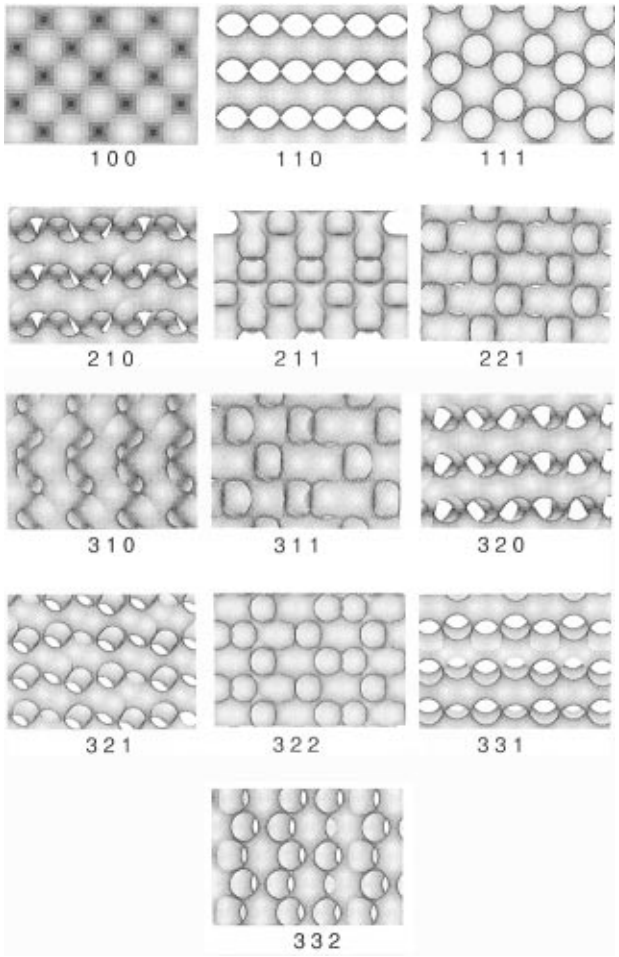

Figure 9. Two-dimensional opaque orthographic projections of D onto a plane. The number below each projection is the corresponding Miller plane index.

In other words, *half of all the symmetry operations in $Im\bar{3}m$ can be found in $Pn\bar{3}m$ and these symmetry operations define $Pn\bar{3}m$ completely.* Thus, in order to minimize misclassifications of the bicontinuous phase, it is desirable to have as many slices of different orientations as possible.

The *hkl* indices associated with the allowable reflections in these three space groups are permutable, e.g., (321) = (312) = (231).[46] However, (*hkl*) for the calculated figures (that could represent SEM photos) has a different interpretation from traditional Miller plane slices. First, all (*hkl*) values are permissible. To illustrate, the (210) face that is a forbidden reflection for all three space groups is allowed in microscopy. Secondly, for a given (*hkl*) face, the slice obtained will generally be different from (*nh nk nl*), where n is an integer. For example, the P(300) slice is not identical to the P(100) slice. In practice however, only a few such slices need to be computed as the 2-D projections quickly show the symmetries involved. These peculiarities arise because the dimension of the unit cells are generally of the order of several nanometers. The slices have classical dimensions such that (*nh nk nl*) is not just the *n*th harmonic of (*hkl*) but resulted from the plane defined by its intersections {1/*nh*, 0, 0}, {0, 1/*nk*, 0}, {0, 0, 1/*nl*} with the crystallographic axes.

The computed slices from surfaces D, G, and P are rendered opaque, similar to what might be observed by SEM. When rendered translucent and subjected to ray-tracing methods, these surfaces resemble TEM micro-

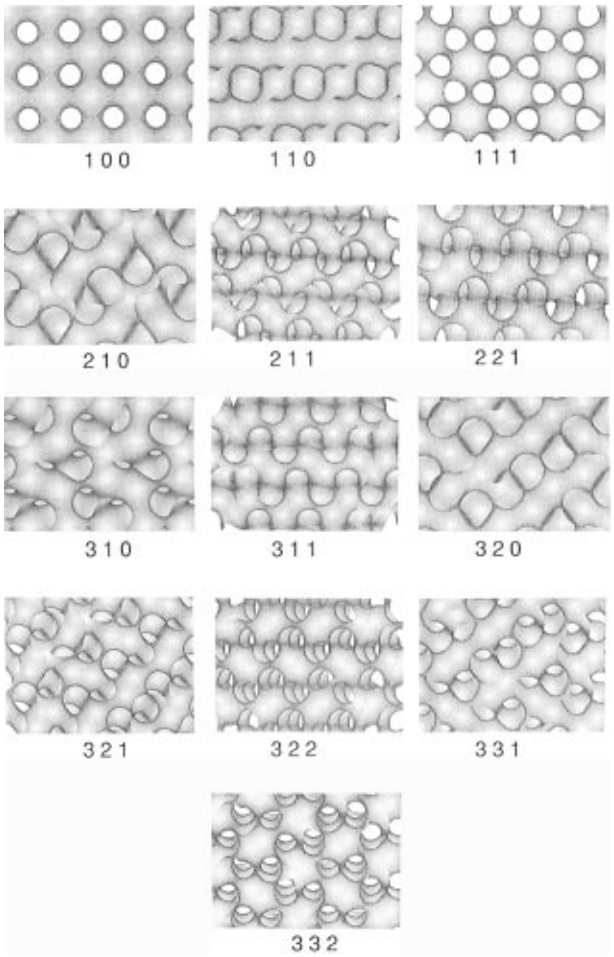

Figure 10. Two-dimensional opaque orthographic projections of G onto a plane. The number below each projection is the corresponding Miller plane index.

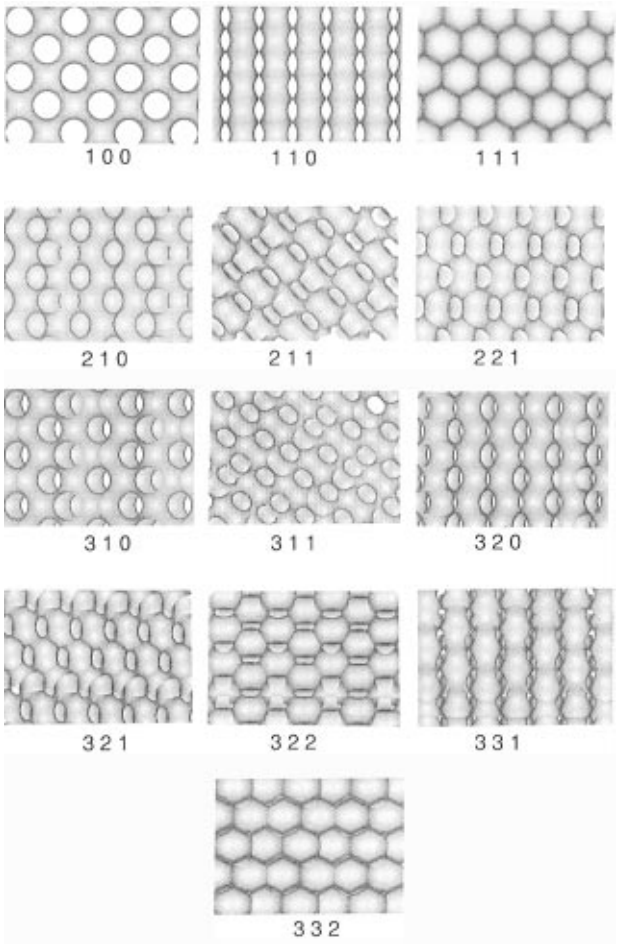

Figure 11. Two-dimensional opaque orthographic projections of P onto a plane. The number below each projection is the corresponding Miller plane index.

graphs.[47] Figure 12 shows one such simulation.[48,49] Similar calculations (using the Fourier series) to simulate TEM micrographs have also been attempted by several workers and the agreement with experimentally obtained slices remarkable; hence, they will not be reproduced in this paper.[50−52] It is not surprising that SEM simulation resembles TEM to some extent since SEM reveals structures along the plane of the surface while TEM reveals a section of the object that is in focus for the camera.

Lately there is increasing interest in the use of electron tomography to characterize the morphologies of block copolymers.[26,53] As is readily apparent from the computed slices, 2-D projections may be misleading. For example, P(111) could easily be mistaken for a hexagonally-packed cylinder. We have created a library of computed 3-D tomographs based on the three minimal surfaces D, G, and P. Figure 13 shows some examples of computed tomographs that could be compared to those obtained experimentally.[34]

In spite of the fact that the minimal surfaces D, G, and P are good representations for some of the phases recently observed in block copolymers, it should kept in mind that minimal surfaces are idealizations of the bicontinuous cubic morphologies. In reality, global equilibration of the bicontinuous cubic phases is difficult to achieve, and some distortions arise from sample preparations.[54] Moreover, real surfaces possess finite thickness. Experimental data seem to indicate that the thickness is variable.[34] It is still unclear whether the variable thickness is best described in terms of a

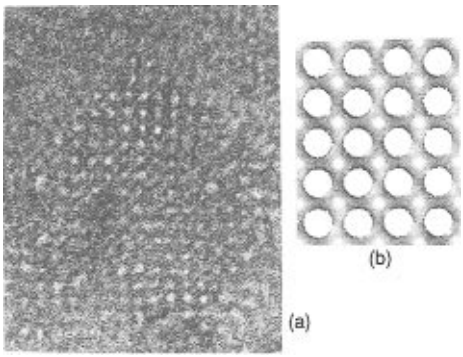

Figure 12. (a) Cryo-TEM of a 3:1 molar mixture of a certain phosphoethanolamine: phosphocholine mixture.[49] (b) Simulated P(100) slice. The simulated holes seem larger because the minimal surface has been given zero thickness.

constant mean curvature, the Gaussian curvature, the constant equipotential surface, or some still unknown parameter.[55,56] Minimal surfaces serve as a starting point by which to study to the rich polymorphism of the block copolymers and amphiphile/water system.

Conclusion

Block copolymers and amphiphile/water systems are similar in the sense that their constituent components tend to self-aggregate (e.g., B blocks with B blocks and hydrophobic tails with hydrophobic tails). Such aggregation creates interesting morphologies that are best understood by their associated minimal surfaces, pro-

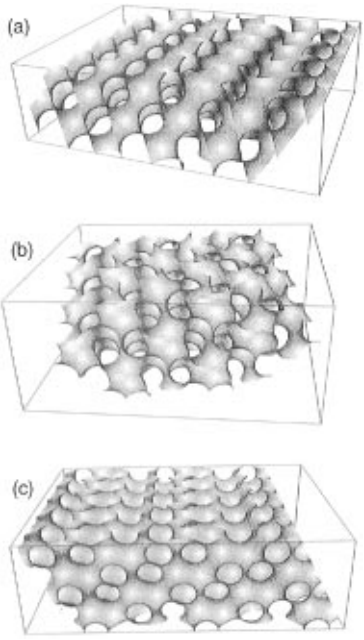

Figure 13. Selected slices of the minimal surfaces (a) D(320), (b) G(331), and (c) P(210). The number in parentheses is the corresponding Miller plane index. Each slice is two unit cells thick.

duced as a consequence of minimizing interfacial contacts between dissimilar components. In particular, the structural details and relationships of the minimal surfaces D, G, and P (associated with the bicontinuous cubic phases $Pn\bar{3}m$, $Ia\bar{3}d$, and $Im\bar{3}m$) are clarified in terms of topological transformations that could account for the qualitative behavior of the phase diagrams. Their 2-D projections reveal remarkable similarities between different cubic phases. Opaque orthographic 2-D projections are analogous to experimental SEM micrographs. Tomographs may also be generated computationally and compared with those obtained experimentally.

Acknowledgment. The authors thank NSF-CTS for support of this research. We also thank Prof. Nick Ercolani (University of Arizona, Mathematics Department) for helpful clarifications on general aspects of differential geometry and Dr. Mike Bruck (University of Arizona Chemistry Department) for discussions on X-ray crystallography.

References and Notes

(1) Odian, G. *Principles of Polymerization;* 3rd ed.; John Wiley & Sons, Inc.: New York, 1991.
(2) Hamley, I. W.; Koppi, K. A.; Rosedale, J. H.; Bates, F. S.; Almdal, K.; Mortensen, K. *Macromolecules* **1993**, *26*, 5959−5970.
(3) Hamley, I. W.; Gehlsen, M. D.; Khandpur, A. K.; Koppi, K. A.; Rosedale, J. H.; Schulz, M. F.; Bates, F. S.; Almdale, K.; Mortensen, K. *J. Phys. II Fr.* **1994**, *4*, 2161−2186.
(4) Disko, M. M.; Liang, K. S.; Behal, S. K.; Roe, R. J.; Jeon, K. J. *Macromolecules* **1993**, *26*, 2983−2986.
(5) Spontak, R. J.; Fung, J. C.; Braunfeld, M. B.; Sedat, J. W.; Agard, D. A.; Ashraf, A.; Smith, S. *Macromolecules* **1996**, *29*, 2850−2856.
(6) Winey, K. I.; Thomas, E. L.; Fetters, L. J. *Macromolecules* **1992**, *25*, 422−428.
(7) Thomas, E. L.; Alward, D. B.; Kinning, D. J.; Martin, D. C.; Handlin Jr., D. L.; Fetters, L. J. *Macromolecules* **1986**, *19*, 2197−2202.
(8) Hajduk, D.; Harper, P. E.; Gruner, S. M.; Honeker, C. C.; Kim, G.; Thomas, E. L.; Fetters, L. J. *Macromolecules* **1994**, *27*, 4063−4075.
(9) Seddon, J. M. *Biochim. Biophys. Acta* **1990**, *1031*, 1−69.
(10) Lindblom, G.; Rilfors, L. *Biochim. Biophys. Acta* **1989**, *988*, 221−256.
(11) Longley, W.; McIntosh, T. J. *Nature* **1983**, *303*, 612−614.
(12) Wennerstrom, H.; Evans, D. F. *The Colloidal Domain: where Physics, Chemistry, Biology, and Technology Meet*; VCH Publishers: New York, 1994.
(13) Actually, it is χN, where N is the degree of polymerization.
(14) Schulz, M. F.; Khandpur, A. K.; Bates, F. S.; K., A.; Mortensen, K.; Hajduk, D. A.; Gruner, S. M. *Macromolecules* **1996**, *29*, 2857−2867.
(15) Bates, F. *Annu. Rev. Phys. Chem.* **1990**, *41*, 525−557.
(16) Helfrich, W. *Z. Naturforsch., C* **1973**, *28*, 693.
(17) Deuling, H. J.; Helfrich, W. *J. Phys. (Paris)* **1976**, *37*, 1335.
(18) k_c is the bending rigidity constant, while λ is a Lagrange multiplier accounting for the area constraint. The free energy is also called the curvature or shape energy, i.e., the energy assigned to the shape of the object or system. The stability of the selected shapes arising from fluctuations has been dealt with elsewhere, e.g., see Helfrich's work.
(19) Anderson, D. M.; Gruner, S. M.; Leibler, S. *Proc. Natl. Acad. Sci. U.S.A.* **1988**, *85*, 5364−5368.
(20) Hoffman, D. *Math. Intelligencer* **1987**, *9*, 8−21.
(21) Mariani, P.; Luzzati, V.; Delacroix, H. *J. Mol. Biol.* **1988**, *204*, 165−189.
(22) Lindblom, G. In *Advances in Lipid Methodology*; Christie, W. W., Ed.; Oily Press: Dundee, 1996; Vol. 3; pp 133−209.
(23) Hajduk, D. A.; Harper, P. E.; Gruner, S. M.; Honeker, C. C.; Thomas, E. L.; Fetters, L. J. *Macromolecules* **1995**, *28*, 2570−2573.
(24) Fontell, K. *Adv. Colloid Interface Sci.* **1992**, *41*, 127−147.
(25) Briggs, J.; Caffrey, M. *Biophys. J.* **1994**, *67*, 1594−1602.
(26) Frank, J. *Three-Dimensional Electron Microscopy of Macromolecular Assemblies*; Academic Press, Inc.: San Diego, CA, 1996.
(27) Wolfram, S. *Mathematica: A System for Doing Mathematics by Computer*; Addison-Wesley Publishing Co.: Redwood City, CA, 1991.
(28) Software Development Group, The Geometry Center: Minnesota, 1993.
(29) Molecular Simulations Incorporated: San Diego, CA, 1994.
(30) Nitsche, J. C. C. *Lectures on Minimal Surfaces*; Cambridge University Press: Cambridge, England, 1989; Vol. 1.
(31) Dierkes, U.; Hildebrandt, S.; Kuster, A.; Wohlrab, O. *Minimal Surfaces I*; Springer-Verlag: Berlin, 1992.
(32) Osserman, R. *A Survey of Minimal Surfaces*; Van Nostrand Reinhold Company: New York, 1969.
(33) Luzzati, V.; Vargas, R.; Mariani, P.; Gulik, A.; Delacroix, H. *J. Mol. Biol.* **1993**, *229*, 540−551.
(34) Spontak, R. J.; Fung, J. C.; Braunfeld, M. B.; Sedat, J. W.; Agard, D. A.; Kane, L.; Smith, S. D.; Satkowski, M. M.; Ashraf, A.; Hajduk, D. A.; Gruner, S. M. *Macromolecules* **1996**, *96*, 4494−4507.
(35) Wells, A. F. *Three-Dimensional Nets and Polyhedra*; John Wiley & Sons: New York, 1977.
(36) The first number denotes the shortest circuit, while the second number is the valence of the vertex.
(37) Seddon, J. M.; Hogan, J. L.; Warrender, N. A.; Pebay-Peyroula, E. *Prog. Colloid Polym. Sci.* **1990**, *81*, 189−197.
(38) Without "tearing" means that the surface remained continuous.
(39) In mathematical terms, a surface without intersections is said to be embedded.
(40) Schoen, A. H. *NASA Tech. Note* **1970**, *D-5541*, 1−98.
(41) This is closely related to page 31 of ref 35.
(42) A simplified analysis goes as follows: In order for the labyrinth net (6,4) to be transformed to (10,3)a, the tetrahedral vertices of the former should be transformed into the trigonal vertices of the latter. Moreover, circuit 6 of the former should also be transformed into circuit 10 of the latter. This is achieved by noting that the probability of a circuit 6 expanding into a greater circuit by random "pulling apart" of the tetrahedral vertices to form two trigonal vertices is $^2/_3$. Thus, upon such "random" pulling apart of the (6,4) labyrinth net (of the D surface), the resultant total number of vertices per circuit is = (2/3 enlargement/vertex)(6 vertex/circuit)(1 new vertex generated/enlargement) + 6 old vertex/circuit = 10 resultant vertex/circuit—which is the (10,3)a labyrinth (corresponding to the G surface).
(43) Similar analysis as above shows that the "random" pulling apart of the (4,6) labyrinth net (of the P surface), the resultant total number of vertices per circuit is = (6/8 enlargement/vertex)(4 vertex/circuit)(2 new vertex generated/enlargement) + 4 old vertex/circuit = 10 resultant vertex/circuit—which is the (10,3)a labyrinth (corresponding to the G surface).

(44) Hyde, S. T.; Andersson, S.; Ericsson, B.; Larsson, K. *Z. Kristallogr.* **1984**, *168*, 213−219.
(45) Hyde, S. T.; Anderson, S. *Z. Kristallogr.* **1985**, *170*, 225−239.
(46) *International Tables for Crystallography;* Hahn, T., Ed.; D. Reidel Publishing Company: Dordrecht, The Netherlands, 1983; Vol. A.
(47) Anderson, D. M.; Bellare, J.; Hoffman, J. T.; Hoffman, D.; Gunther, J.; Thomas, E. L. *J. Colloid Interface Sci.* **1992**, *148*, 398−414.
(48) As noted earlier, to unambiguously identify a particular bicontinuous cubic phase requires several slices.
(49) Lee, Y. S.; Yang, J. Z.; Sisson, T. M.; Frankel, D. A.; Gleeson, J. T.; Aksay, E.; Keller, S. L.; Gruner, S. M.; O'Brien, D. F. *J. Am. Chem. Soc.* **1995**, *117*, 5573−5578.
(50) Deng, Y.; Landh, T. *Zool. Studies* **1995**, *34 Supplement 1*, 175−177.
(51) Landh, T. *Zool. Studies* **1995**, *34 Supplement 1*, 241−244.
(52) Landh, T. *FEBS Lett.* **1995**, *369*, 13−17.
(53) Frank, J. *Electron Tomography*; Plenum Press: New York, 1992.
(54) Sawyer, L. C.; Grubb, D. T. *Polymer Microscopy*; Chapman and Hall, Ltd.: London, 1987.
(55) von Schnering, H. G.; Nesper, R. *Angew. Chem., Int. Ed. Engl.* **1987**, *26*, 1059−1200.
(56) Andersson, S.; Hyde, S. T.; Larsson, K.; Lidin, S. *Chem. Rev.* **1988**, *88*, 221−242.

MA9614353